ChemComm

COMMUNICATION

View Article Online
View Journal | View Issue



Cite this: *Chem. Commun.*, 2024, **60**, 7073

Received 19th April 2024,
Accepted 28th April 2024

DOI: 10.1039/d4cc01868k

rsc.li/chemcomm



# Regulating iminophosphorane P=N bond reactivity through geometric constraints with cage-shaped triarylphosphines†

Lei Hu,‡§[ab] Sayandip Chakraborty,§[a] Nikolay Tumanov,[a] Johan Wouters,[a] Raphaël Robiette *[b] and Guillaume Berionni *[a]

**Structure–reactivity investigations and quantum-chemical parametrization of steric and electronic properties of geometrically constrained iminophosphoranes enabled the design of new frustrated Lewis pairs and revealed unusual properties at the phosphonium center embedded in the cage-shaped triptycene tricyclic scaffold.**

Iminophosphoranes, the nitrogen analogues of phosphorus ylides in aza-Wittig reactions,[1] are increasingly used to design pincer type ligands for transition-metals[2] and main-group elements.[3] They have found recent applications in organocatalysis[4] and in the phosphine-mediated redox catalyzed Staudinger ligation of carboxylic acids and azides (Scheme 1a).[5] Iminophosphoranes are prepared by the Staudinger reaction,[1a] whose reaction intermediates have been extensively investigated (Scheme 1b).[6]

Owing to the high basicity of their nitrogen atom, iminophosphoranes have been extensively used to design superbases (*e.g.* Schwesinger phosphazenes),[7] and have been combined with bulky boron Lewis acids such as $B(C_6F_5)_3$ to generate frustrated Lewis pairs (FLPs) reacting with small molecules such as $CO_2$ and $H_2$ (Scheme 1c).[8]

Whereas the reactivity of these phospha-aza ylides is usually governed by the electronic and steric properties of the substituents at the P and N atoms, constraining their geometry with a highly strained skeleton or cage-shaped framework is of increasing interest for modulating the reactivity of p-block compounds and reaching new reactivities (Scheme 2).[9]

Chitnis and coworkers recently designed phosphaza-adamantane with thermal, air, and redox stability by using a geometrically constrained adamantane scaffold (Scheme 2a-A).[10] Radosevich and coworkers modulated the properties of the P=N bond in phosphazenes by designing phosphabicyclic compounds with distorted T-shaped molecular geometries, enabling the tuning of their reactivity *via* a geometric constraint (Scheme 2a-B).[11] Uchiyama recently employed a phospha-boratriptycene cage-shaped scaffold to intercept betaine intermediates in Wittig reactions of phosphorus ylides with aldehydes (Scheme 2a-c).[12]

We now report a series of phosphatricyclic nitrogen-ylides derived from 9-phosphatriptycene,[13] in which the geometric constraint is inducing an unusual pyramidalized phosphorus environment at the edge of the triptycene scaffold.[14] The impact of the geometrical constraint on the Lewis and Brønsted basicities, steric hindrance and reactivity of the P=N bond was elucidated by quantitative investigations of their association with carbenium ions, and Brønsted and Lewis acids.

Adducts featuring unprecedented non-covalent fluorine or oxygen non-covalent bonding to C–P σ* orbitals were obtained

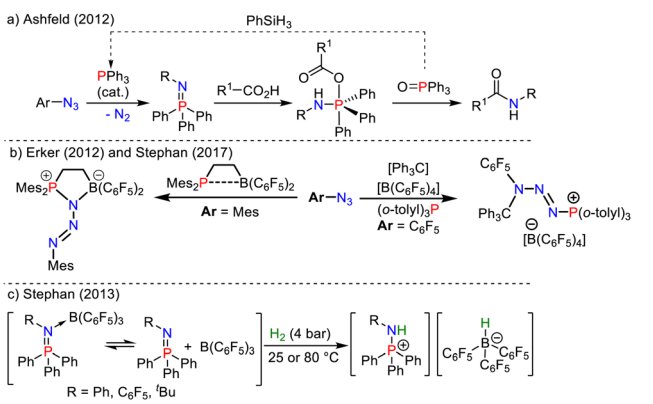


Scheme 1 (a) $P^{III}/P^{V}$-redox catalyzed Staudinger ligation reaction.[5] (b) Interrupted Staudinger reactions.[6] (c) Applications of iminophosphoranes in FLP chemistry.[8]

[a] *Université de Namur, Department of Chemistry, Namur Institute of Structured Matter (NISM), Rue de Bruxelles 61, Namur 5000, Belgium. E-mail: guillaume.berionni@unamur.be*

[b] *Université Catholique de Louvain, Institute of Condensed Matter and Nanosciences, Place Louis Pasteur 1 box L4.01.02, Louvain-la-Neuve 1348, Belgium. E-mail: raphael.robiette@uclouvain.be*

† Electronic supplementary information (ESI) available. CCDC 2313762–2313774 and 2347266–2347270. For ESI and crystallographic data in CIF or other electronic format see DOI: https://doi.org/10.1039/d4cc01868k

‡ Current address: Xiamen Key Laboratory of Marine Medicinal Natural Product Resources, Xiamen medical college, Xiamen 361023, P. R. China.

§ These authors contributed equally to this work.

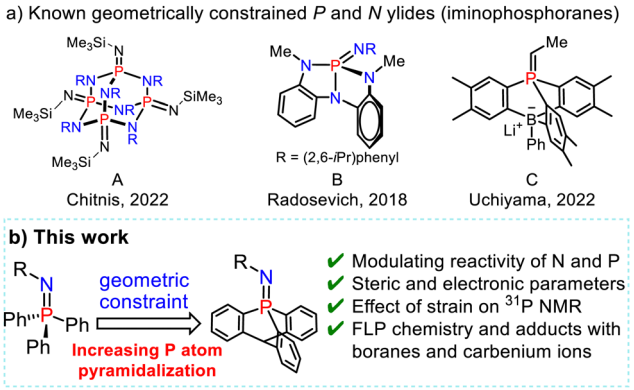


Scheme 2 (a) Examples of geometrically constrained phosphorus frameworks. (b) This work: exploiting geometric distortion at phosphorus to modulate the P=N bond reactivity and steric hindrance.

and the striking reactivities of the cage-shaped phosphinimines were further exploited to design FLPs with bulky Lewis acids.

We first compared the magnetic and structural properties of triphenylphosphine **2–4** and triptycene chalcogenides **6–8** (Table 1). Single-crystal X-ray diffraction analysis revealed that TripP=E derivatives **6–8** exhibited a larger pyramidalization angle $\alpha$ than in classical $Ar_3P$=E derivatives **2–4**, corresponding to larger CPC angles of 107.7° *versus* 97.7°. In $^{31}$P NMR spectroscopy, a large shielding is observed between the 9-phosphatriptycene **5** (−64.4 ppm) and $Ph_3P$ **1** (−4.7 ppm), while a smaller shielding was observed between Trip-P=E and $Ph_3P$=E derivatives (Table 1). Consistent with the literature,[14e] the $^1J$ $^{31}$P–$^{77}$Se of 822 Hz in **8** is nearly 100 Hz larger than for $PPh_3$=Se **4** (729 Hz) indicating that the overall donating ability of phosphatriptycene **5** is less than $Ph_3P$.[13a] Compound **6** was found to stabilize a molecule of $H_2O_2$ (Fig. S1 in the ESI†).

We then performed the Staudinger reactions of 9-phosphatriptycene **5** with several azides R–$N_3$ to synthesize the cage-shaped iminophosphoranes **9–14** (Scheme 3). According to the classical mechanism,[15] these reactions are likely proceeding *via*

Table 1 Phosphorus-element bond lengths (in Å), pyramidalisation at the P atom (angle $\alpha$ in °) and $^{31}$P NMR chemical shifts ($\delta$ in ppm) in triphenylphosphine **1–4** and phosphatriptycene **5–8** derivatives

| Chalcogenide derivatives with *E* = | | O | S | Se |
|---|---|---|---|---|
| Triphenylphosphine | **1** | **2** | **3** | **4** |
| 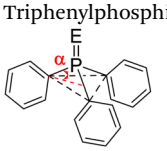 | P–E | — | 1.482 (3) | 1.955 (7) | 2.114 (8) |
| | $\alpha^a$ | 26.1[14a] | 22.4[14b] | 22.9[14d] | 22.6[14g] |
| | $\delta$ $^{31}$P ppm | −4.7 | 29.2[14c] | 43.3[14e] | 35.3[14f] |
| Phosphatriptycene | **5** | **6** | **7** | **8** |
| 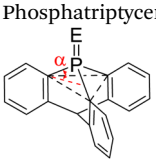 | P–E | — | 1.482 (1) | 1.941 (1) | 2.091 (1) |
| | $\alpha$ | 29.8 | 28.7 | 29.2 | 29.1 |
| | $\delta$ $^{31}$P ppm | −64.4[14h] | 7.32 | 12.72 | 4.52 |

[a] Pyramidalization angle $\alpha$ defined as the angle between the C–P bonds and the plane formed by the *ipso*-carbon atoms of the triptycene aryl rings, see ESI.

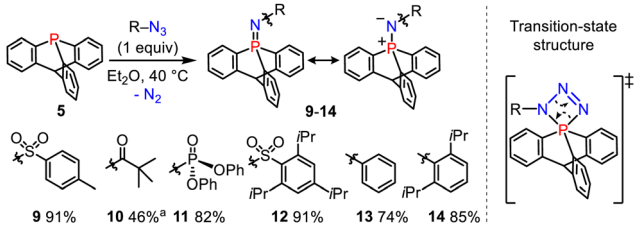


Scheme 3 Synthesis of the 9-phosphatriptycene-imines **9–14**. [a] Prepared with different synthetic procedures, see the ESI† for more details.

an unusual inorganic spiro-cyclic transition-state with a four-membered PNNN ring connected to a phosphabicyclo[2.2.2]-octane tricyclic core.

The $^{31}$P NMR chemical shifts of **9–14** (−5 to −33 ppm) were again more shielded than in the corresponding $Ph_3P$=NR derivatives reported in the literature (0 to 15 ppm).[14] The formal P=N double bond has predominantly an ylidic nature (see right-hand side resonance structure, Scheme 3) as confirmed by NBO calculations showing that the short PN bond lengths are resulting from negative hyperconjugation between the N lone pairs and $\sigma^*_{P-C}$ antibonding orbitals (2nd order perturbation stabilization energy E2 = 9.8, 33.2 and 33.3 kcal mol$^{-1}$ for **13**).[16]

X-ray crystallographic analysis of compounds **9–14** (see ESI†) revealed a high pyramidalization angle at P, *e.g.* $\alpha$ = 29.0° in **13** and only 23.3° for its $Ph_3P$=NPh analogue (Fig. 1a and b).

Compound **10** has a P···O distance (2.717(3) Å) well under the van der Waals radii of both atoms (represented by the red and yellow wireframe spheres around O and P, respectively, Fig. 1c), implying a preponderant resonance structure with marked electrostatic interaction between the positively charged P atom and negatively charged O atom (Fig. 1d).

This interaction is also confirmed by the NBO analysis of **10**, which reveals an electronic interaction between one lone pair of the oxygen atom and one $\sigma^*_{P-C}$ bond (E2 = 2.2 kcal mol$^{-1}$). Due to the cage-shaped structure of phosphatriptycene, this P-distance is significantly shorter than in any previous reported

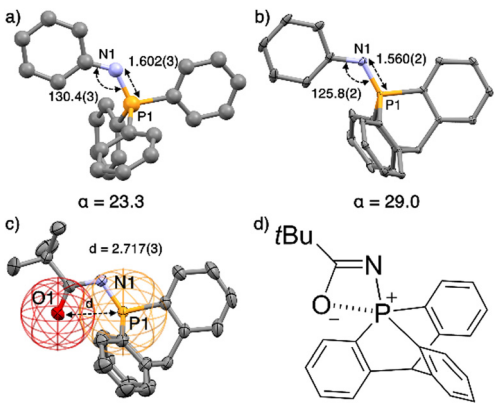


Fig. 1 (a) Structure of $Ph_3P$=NPh[17e,f] and (b) of its analogue 13 with key geometrical features. (c) Ellipsoid representation of single crystal X-ray structures of 10; H atoms and solvent are omitted for clarity. (d) Preponderant mesomeric structure of 10. Distances in Å, angles in °, pyramidalization angle $\alpha$ in °.

 

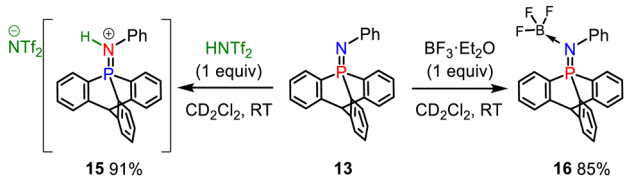


Scheme 4 Reaction of **13** with a Brønsted and a boron Lewis acid.

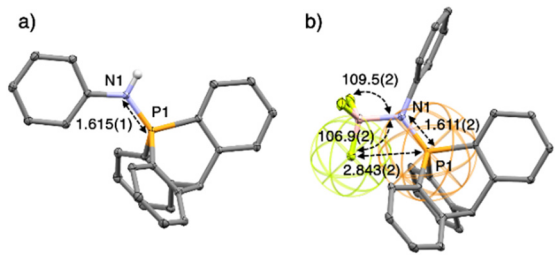


Fig. 2 Ellipsoid representation (50% probability level) of single-crystal X-ray structures of one of the two molecules in the asymmetric unit of **15** (a), and **16** (b). H atoms, anion and solvent are omitted for clarity.

phosphorus imidates (previous shortest = 2.848(2) Å for the corresponding $Ph_3P{=}NCOtBu$ analogue of **10**).[17]

The iminophosphorane **13** was used for subsequent reactivity studies and was reacted with triflimidic acid $HNTf_2$ and $BF_3{\cdot}OEt_2$ giving respectively **15** and **16** in good yields (Scheme 4). Protonation and $BF_3$ complexation induced a deshielding of the $^{31}P$ NMR signals of **15** (10.7 ppm) and **16** (10.4 ppm) compared to that of **13** (−20.4 ppm). Crystallographic analysis showed that $H^+$ and $BF_3$ complexation of **13** resulted in a significant P–N lengthening, with a PN distance of 1.560(2) Å in **13**, 1.615(1) Å in **15** and 1.611(2) Å in **16** (Fig. 2). This can be accounted for by the loss of one lone pair on the nitrogen that decreases the hyperconjugation with the $\sigma^*_{P-C}$ orbitals (E2 = 13.3 and 13.5 kcal $mol^{-1}$ for **15**) as compared to what was observed in **13** (*vide supra*).

The structure of **16** in the solid state revealed that one F atom in $BF_3$ is anti ($\theta_{C-P-F}$ = 173.65(8)°) to one of the P–$C_{arom}$ bonds (Fig. 2b). The valence angle $\theta_{N-B-F}$ for $F_1$ is 106.9(2)°, whereas it is 109.5(2)° and 109.8(2)° for the other two fluorine atoms. This suggests an interaction between the lone pair of one fluorine with the σ* orbital of one $C_{arom}$–P bond. This P···F distance of 2.8433(14) Å is longer than in the phosphonium based anion receptors of Gabbaï (2.666(2) Å) in which the phosphonium bears a positive charge.[18] Nevertheless, it is still very short with a F···P distance in **16**, well below the sum of the van der Waals radii of both atoms (3.35 Å), represented by wireframe coloured spheres around F and P (Fig. 2b).

Then, the association of **13–14** with tris(pentafluorophenyl)-borane **17** was investigated by multinuclear NMR spectroscopy (Scheme 5). When mixing these reagents in $CDCl_3$, a negligible deshielding of the signal of **13** (≈3 ppm) was observed by $^{31}P$ NMR spectroscopy, and only a broadening of the peaks was observed in $^1H$ NMR, while the $^{11}B$ NMR signal of **17** remained at −60.0 ppm. This indicated a very weak interaction between **13** and $B(C_6F_5)_3$ typical of an encounter complex or a frustrated

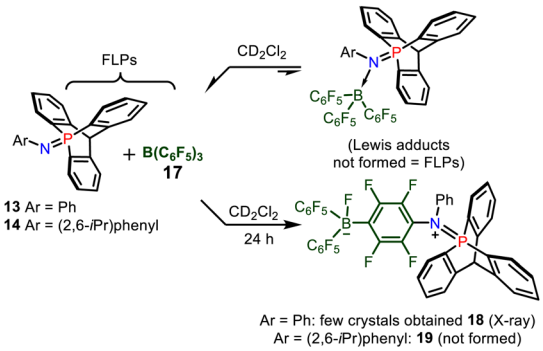


Scheme 5 FLPs between **13** and **17** and deactivation pathway resulting in the formation of the phospha-iminium fluoroborate **18**.

Lewis pair, and the formation of a Lewis adduct was thus excluded. After keeping the FLP solution for one day, crystals of compound **18** were obtained (see ESI,† Fig. S2) among other decomposition products. Thus, the deactivation of FLP occurs partly *via* $S_NAr$ reaction of the nitrogen atom of the 9-phospatriptycene imine **13** at the para position of a $C_6F_5$ ring of $B(C_6F_5)_3$ (Scheme 5), similarly as with phosphorus ylides.[8c] In the case of **14**, since it is of larger steric hindrance around it's nitrogen atom, such type of $S_NAr$ reaction to yield **19** was not possible.

The steric hindrance at the nitrogen atom was comparable for TripP=NPh (**13**) and $Ph_3P{=}NPh$ according to their similar buried volume $\%V_{bur}$ and $He_8$_steric parameters (see ESI,† Table S3).[19] Analogously, the $\%V_{bur}$ of phosphatriptycene **5** (31.3%) is comparable to that of $Ph_3P$ **1** (29.6%).[20]

Computations show that the proton (PA) and methyl cation affinities (MCA) of iminophosphoranes **9–14** are influenced by geometric constraints at the phosphorus atom. This constraint decreases the basicity at N by up to 8 kcal $mol^{-1}$ when comparing **13** to is analogue $Ph_3P{=}NPh$ (Table 2). It simultaneously enhances the Lewis acidity at the phosphorus atom by 4 kcal $mol^{-1}$, as evidenced by fluoride ion affinity (FIA) values at the electron deficient formal phosphonium P centre. Analysis of the fluoride complexation through the activation strain model (see ESI,† Table S4) indicates that this enhanced Lewis acidity is mainly due to a lower distortion energy in the case of **13**. The energy necessary for the geometrically constrained phosphatriptycene imine structure to adopt the trigonal

Table 2 Computed proton affinities (PAs) and methyl cation affinities (MCAs) of **9–14** with respect to the N atom in benzene as a solvent in kcal $mol^{-1}$, and fluoride ion affinities (FIA) in kcal $mol^{-1}$ with respect to the P atom

| | Cmpd B | 9 | 10 | 11 | 12 | 13 | 14 | $Ph_3P{=}NPh$ |
|---|---|---|---|---|---|---|---|---|
| PA | 263 | 247 | 255 | 246 | 245 | 262 | 264 | 270 |
| MCA | 110 | 93 | 95 | 92 | 94 | 108 | 113 | 113 |
| FIA[a] | 60[b] | 47 | 37 | 45 | 51 | 36 | 38 | 32 |

[a] Computed FIA at the pseudo phosphonium center using the isodesmic approach with $COF_2$ anchor points; see ESI, Table S2 for the $FSiMe_3$ anchor point and for FIAs for **6–8**. [b] In agreement with the reported FIA value for compound **B** (Radosevich T-shaped iminophosphoranes shown in Scheme 2b) of 57 kcal $mol^{-1}$ in ref. 11.

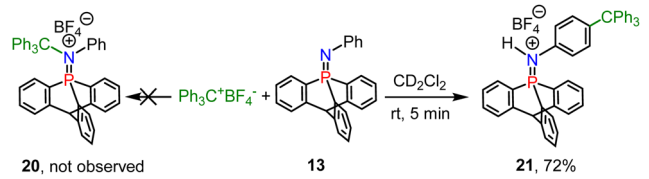


Scheme 6 FLP type reaction of iminophosphorane **13** with the tritylium tetrafluoroborate to yield compound **21**.

bipyramidal geometry is indeed lower (by 4.6 kcal $mol^{-1}$) than the one required for $Ph_3P{=}NPh$.

Finally, we found that combining **13** with a titylium ion results in a nitrogen/carbon FLP, and the phospha-iminium **20** was not formed (Scheme 6), but instead $S_EAr$ reactions occurred at the para position of N-Ph of **13** to yield compound **21**, evidenced by X-ray diffraction (Fig. S2b, ESI†).

Thus, in conclusion, the geometric constraints brought by the cage-shaped tricyclic phosphatriptycene scaffold decrease the Brønsted basicity at the nitrogen but enhance the Lewis acidity at the phosphorus, leading to a partial Umpolung type reactivity at the P=N bond. Unusually short non-covalent F···P and O···P intramolecular electrostatic contacts also result from the geometrical constraints. The new cage-shaped phosphatriptycene nitrogen-ylides might have interesting reactivity in terms of frustrated Lewis pairs catalysis[21] which is subject to further exploration in our labs. The transition metal-free directed electrophilic borylation[22] of the triptycene core based on the N-centred directing group approach is also under investigation.

We acknowledge the University of Namur (CERUNA PhD fellowship for S. C.) and the Fond de la Recherche Scientifique FNRS (F.R.S-FNRS) for financial support (Grants T.0012.21 (G. B.) and GEQ UG02222F (J. W.)). Computational resources have been provided by the supercomputing facilities of the Université catholique de Louvain (CISM/UCLouvain) and the Consortium des Équipements de Calcul Intensif en Fédération Wallonie Bruxelles (CÉCI) funded by the F.R.S.-FNRS under convention 2.5020.11 and by the Walloon Region. We thank the PC2 (UNamur) technological platforms for access to all characterization instruments. LH expresses gratitude for the PhD grant support from the China Scholarship Council (CSC, no. 201606670003) and acknowledges the FNRS Mobility Grant for research exchange at the University of Basel. Special appreciation goes to Prof. Olivier Baudoin for hosting and to Dr A. Clemenceau for experimental assistance during this period. RR is a Maître de Recherche of the F.R.S.-FNRS.

## Conflicts of interest

There are no conflicts of interest to declare.

## Notes and references

1 (*a*) H. Staudinger and J. Meyer, *Helv. Chim. Acta*, 1919, **2**, 635–646; (*b*) S. P. Marsden, *et al.*, *Org. Lett.*, 2008, **10**, 2589–2591; (*c*) L. Wang, *et al.*, *Synthesis*, 2015, 3522–3528; (*d*) H. A. Van Kalkeren, *et al.*, *Adv. Synth. Catal.*, 2012, **354**, 1417–1421; (*e*) H. A. Van Kalkeren, *et al.*, *Eur. J. Org. Chem.*, 2013, 7059–7066; (*f*) H. Bel Abed, *et al.*, *Org. Biomol. Chem.*, 2014, **12**, 7159–7166.
2 (*a*) L. Beaufort, *et al.*, *J. Mol. Catal. A: Chem.*, 2008, **283**, 77–82; (*b*) O. Alhomaidan, *et al.*, *Organometallics*, 2008, **27**, 6343–6352; (*c*) E. Martinez-Arripe, *et al.*, *Organometallics*, 2012, **31**, 4854–4861; (*d*) J. García-Álvarez, *et al.*, *J. Organomet. Chem.*, 2014, **751**, 792–808.
3 (*a*) T. Cantat, *et al.*, *Dalton Trans.*, 2008, 1957–1972; (*b*) M. Fustier-Boutignon, *et al.*, *Chem. Rev.*, 2019, **119**, 8555–8700; (*c*) K. Dehnicke and F. Weller, *Coord. Chem. Rev.*, 1997, **158**, 103; (*d*) D. W. Stephan, *Adv. Organomet. Chem.*, 2006, **54**, 267.
4 D. Rozsar, *et al.*, *Angew. Chem., Int. Ed*, 2023, **62**, e202303391.
5 A. D. Kosal, *et al.*, *Angew. Chem., Int. Ed.*, 2012, **21**, 12036–12040.
6 (*a*) A. Stute, *et al.*, *Chem. Commun.*, 2012, **48**, 11739–11741; (*b*) J. Zhou, *et al.*, *Dalton Trans.*, 2017, **46**, 9334–9338.
7 (*a*) M. Formica, *et al.*, *Acc. Chem. Res.*, 2020, **53**, 2235–2247; (*b*) R. Schwesinger, *et al.*, *Angew. Chem., Int. Ed. Engl.*, 1993, **32**, 1361.
8 (*a*) C. F. Jiang and D. W. Stephan, *Dalton Trans.*, 2013, **42**, 630–637; (*b*) J. Y. Zhang, *et al.*, *Chin. Chem. Lett.*, 2018, **29**, 1226–1232; (*c*) S. Döring, *et al.*, *Organometallics*, 1998, **17**, 2183–2187.
9 (*a*) T. S. Barnard and M. R. Mason, *Organometallics*, 2001, **20**, 206–214; (*b*) S. Tretiakov, *et al.*, *Angew. Chem., Int. Ed.*, 2021, **60**, 9618–9626; (*c*) For a recent review on p-block compounds see: T. J. Hannah and S. S. Chitnis, *Chem. Soc. Rev.*, 2024, **53**, 764–792.
10 J. Bedard, *et al.*, *Angew. Chem., Int. Ed.*, 2022, **61**, e202204851.
11 Y.-C. Lin, *et al.*, *Chem. Sci.*, 2018, **9**, 4338–4347.
12 (*a*) Y. Uchiyama, *et al.*, *J. Org. Chem.*, 2022, **87**, 15899–15913; For further applications of phosphatriptycenes in catalysis and coordination chemistry, see: (*b*) Y. Cao, *et al.*, *Organometallics*, 2019, **38**, 1868.
13 (*a*) L. Hu, *et al.*, *J. Org. Chem.*, 2019, **84**, 11268–11274; (*b*) H. Gildenast, *et al.*, *Dalton Trans.*, 2022, **51**, 7828–7837; (*c*) D. Rottschäfer, *et al.*, *Inorg. Chem.*, 2023, **62**, 18228; (*d*) For the original synthesis of 9-phosphatriptycene, see: C. Jongsma, *et al.*, *Tetrahedron*, 1974, **30**, 3465–3469.
14 (*a*) H. Kooijman, *et al.*, *Acta Cryst. C*, 1695, **1998**, 54; (*b*) L. R. Falvello, *et al.*, *CSD Commun.*, 2002, CCDC 186887; (*c*) J. Yang, *et al.*, *Chem. Commun.*, 2016, **52**, 12233; (*d*) C. Foces-Foces and A. L. Llamas-Saiz, *Acta Cryst. C*, 1998, **54**, 9800013; (*e*) P. W. Codding and K. A. Kerr, *Acta Crystallogr., Sect. B: Struct. Crystallogr. Cryst. Chem.*, 1978, **34**, 3785; (*f*) R. Kumar, *et al.*, *Eur. J. Inorg. Chem.*, 2018, 1028; (*g*) A. L. Rheingold, *CSD Commun.*, 2011, CCDC 856709; (*h*) H. Hu, *et al.*, *Dalton Trans.*, 2021, **50**, 4772–4777.
15 F. L. Lin, *et al.*, *J. Am. Chem. Soc.*, 2005, **127**, 2686–2695.
16 A similar analysis was made by Dehnicke, See: H. Folkerts, *et al.*, *Angew. Chem., Int. Ed. Engl.*, 1995, **34**, 1362.
17 (*a*) W. Han, *et al.*, *Org. Lett.*, 2022, **24**, 6247–6251; (*b*) C. Larré, *et al.*, *Eur. J. Inorg. Chem.*, 1999, 601–611; (*c*) J. Yang, *et al.*, *Chem. Commun.*, 2016, **52**, 12233; (*d*) Y. Matano, *et al.*, *J. Am. Chem. Soc.*, 2001, **123**, 10954–10965; (*e*) E. Böhm, *et al.*, *Zeit. Naturforsch. B*, 2014, **43**, 138; (*f*) I. Bar and J. Bernstein, *Acta Crystallogr., Sect. B: Struct. Crystallogr. Cryst. Chem.*, 1980, **36**, 1962–1964.
18 T. W. Hudnall and F. P. Gabbaï, *J. Am. Chem. Soc.*, 2008, **130**, 10890–10891.
19 (*a*) N. Fey, *et al.*, *Organometallics*, 2008, **27**, 1372–1383; (*b*) J. Jover, *et al.*, *Organometallics*, 2012, **31**, 5302–5306; (*c*) D. J. Durand and N. Fey, *Chem. Rev.*, 2019, **119**, 6561–6594.
20 H. Clavier and S. P. Nolan, *Chem. Commun*, 2010, **46**, 841–861.
21 M. G. Guerzoni, *et al.*, *Chem. Catal.*, 2022, **2**, 2865–2875.
22 (*a*) S. Rej and N. Chatani, *J. Am. Chem. Soc.*, 2021, **143**, 2920–2929; (*b*) S. A. Iqbal, *et al.*, *Chem. Soc. Rev.*, 2020, **49**, 4564–4591.